

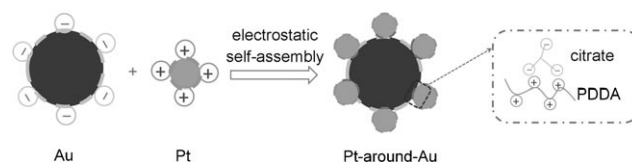
# Electrostatic Self-Assembly of a Pt-around-Au Nanocomposite with High Activity towards Formic Acid Oxidation\*\*

Sheng Zhang, Yuyan Shao, Geping Yin,\* and Yuehe Lin\*

Direct formic acid fuel cells (DFAFCs) have attracted growing attention as a promising power source because of their high energy density, facile power-system integration, and convenient storage and transport of liquid formic acid.<sup>[1–5]</sup> Platinum and palladium are the best-known catalysts for the oxidation of small organic molecules.<sup>[6–12]</sup> For HCOOH oxidation, Pd shows superior initial performance compared to Pt.<sup>[13,14]</sup> However, the high performance cannot be sustained, as Pd dissolves in acidic solutions<sup>[15]</sup> and is vulnerable towards intermediate species.<sup>[16]</sup> For pure Pt, the activity towards HCOOH oxidation is hindered by CO poisoning.<sup>[17]</sup> Modification of Pt with foreign metal has been considered as an effective method to enhance the activity and durability towards HCOOH oxidation.<sup>[3,18,19]</sup>

Heterogeneous bimetallic nanocrystals have demonstrated excellent electrocatalytic activity and durability in fuel cells. Xia and co-workers deposited Pt branches on a Pd core, and the resulting Pd/Pt bimetallic nanodendrites exhibited high activity for oxygen reduction.<sup>[20]</sup> Adzic and co-workers modified Pt nanoparticles (NPs) with Au clusters, which significantly enhanced the stability of Pt.<sup>[21]</sup> Yang et al. localized overgrowth of Pd on cubic Pt seeds, and these binary Pt/Pd nanoparticles showed improved activity towards formic acid oxidation versus pure Pt.<sup>[22]</sup> These bimetallic NPs were all prepared by depositing one nanocluster on the other one, meaning that the active sites are partly shielded at the interface of the two kinds of metal NPs. Herein, we report a novel Pt-around-Au nanocomposite based on the electrostatic self-assembly of oppositely charged NPs. This composite is demonstrated as an excellent electrocatalyst for formic acid oxidation.

Self-assembly of NPs by electrostatic interaction has been investigated in recent years, and it can facilitate the production of many new macroscopic structures.<sup>[23–27]</sup> The interplay of repulsive interactions between NPs with the same charge and attractive interactions between those with opposite charges results in the self-assembly of these NPs into highly ordered structure. In contrast to atomic systems, electrostatic self-assemblies are not limited by charge neutrality, which allows us to obtain a great diversity of new binary structures.<sup>[23]</sup> To our knowledge, this is the first time that the electrostatic self-assembly method has been employed to synthesize Pt/Au binary nanocrystals. The whole process is shown in Scheme 1 (see the Supporting Information for



**Scheme 1.** Synthesis of Pt-around-Au nanocomposite by electrostatic self-assembly. Positively charged Pt NPs are prepared in PDDA solution and negatively charged Au NPs are synthesized in sodium citrate solution.

details). The positively charged Pt NPs are prepared in poly(diallyldimethylammonium chloride) (PDDA) solution,<sup>[28]</sup> while negatively charged Au NPs are synthesized in sodium citrate solution.<sup>[18]</sup> Both types of NPs are stable when kept in separate solutions owing to the presence of stabilizing agents.<sup>[29]</sup> Once these two solutions are mixed, the positively charged Pt NPs interact with the negatively charged Au NPs, and Pt-around-Au nanocomposite particles are obtained.

X-ray diffraction (XRD) patterns (Figure 1) show that both Pt and Au NPs have face-centered cubic (fcc) crystal structure, and particle sizes are calculated (using the Scherrer equation<sup>[30]</sup>) to be about 2.8 and 6.1 nm, respectively. Figure 2 shows the TEM image for highly dispersed Pt-around-Au nanocomposite particles on carbon black (more TEM images are shown in Figure S1 in the Supporting Information). The particle size distributions (Figure S2 in the Supporting Information) combined with energy dispersive X-ray spectroscopy (EDS) analysis (Figure S3 in the Supporting Information) confirm that the larger particles in the TEM images are Au NPs. These Au NPs are surrounded by smaller Pt NPs to form a complex-like structure (similar to the central ion and ligands in coordination chemistry<sup>[26]</sup>) arising from the electrostatic interaction between negatively charged Au NPs and positively charged Pt NPs.<sup>[26,27]</sup> This structure is consistent

[\*] S. Zhang, Prof. G. Yin  
School of Chemical Engineering & Technology  
Harbin Institute of Technology, Harbin, 150001 (China)  
E-mail: yingphit@hit.edu.cn

S. Zhang, Dr. Y. Shao, Dr. Y. Lin  
Pacific Northwest National Laboratory, Richland, WA 99352 (USA)  
E-mail: yuehe.lin@pnl.gov

[\*\*] S.Z. and Y.S. contributed equally to this work. The work was done at Pacific Northwest National Laboratory (PNNL) and was supported by a LDRD program. The characterization was performed using EMSL, a national scientific user facility sponsored by the DOE's Office of Biological and Environmental Research and located at PNNL. PNNL is operated for the DOE by Battelle under Contract DE-AC05-76RL01830. S.Z. acknowledges a fellowship from the China Scholarship Council and PNNL to perform this work at PNNL. G.Y. acknowledges the support from the Natural Science Foundation of China (No. 50872027).

Supporting information for this article is available on the WWW under <http://dx.doi.org/10.1002/anie.200906987>.

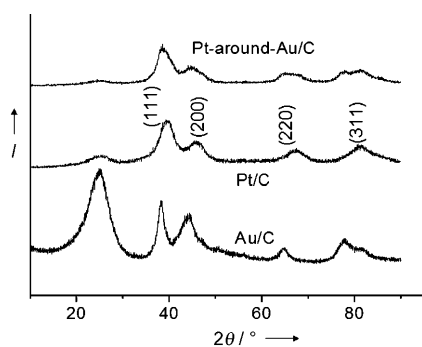


**Figure 1.** X-ray diffraction (XRD) patterns of Pt/C, Au/C, and Pt-around-Au/C.

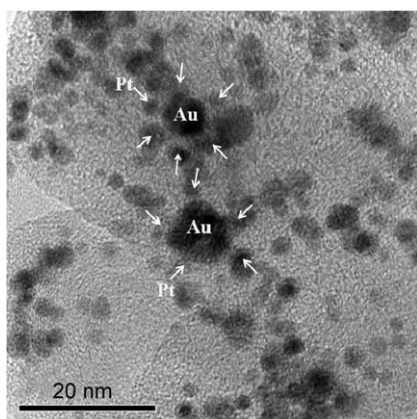


**Figure 2.** TEM image of Pt-around-Au/C. Au NPs (larger particles) are surrounded with Pt NPs (smaller ones) by electrostatic self-assembly.

with the XRD patterns of the Pt-around-Au nanocomposite, which show the coexistence of Pt diffraction peaks and Au diffraction peaks. EDS analysis confirms that the atomic ratio between Au and Pt in the nanocomposite is approximately 1:9. Generally, mixing solutions containing differently charged NPs leads to different results depending on the ratio of the positively and negatively charged particles.<sup>[26]</sup> If comparable amounts of positively and negatively charged NPs are mixed, a 3D ordered solid consisting of NPs will form and aggregate rapidly, because there are not enough net charges to form discrete particles.<sup>[25]</sup> As demonstrated herein, the negatively charged Au NPs and a large excess of positively charged Pt NPs self-assemble into the complex-like structure. The excess positively charged Pt NPs surrounding Au generate electrostatic repulsive interaction.<sup>[25,31]</sup> This repulsion stabilizes the nanocomposite and prevents the formation of precipitate in solution. Therefore, the Pt-around-Au nanocomposite has a uniform distribution on the carbon support.

The electrochemical performance of the Pt-around-Au nanocomposite was evaluated. Typical hydrogen and oxygen adsorption and desorption behavior (Figure 3A) can be clearly detected on Pt-around-Au/C and Pt/C.<sup>[32]</sup> The reduction peak at 1.2 V in the cyclic voltammogram of Pt-around-Au/C confirms the presence of Au.<sup>[33]</sup> The electrochemical surface areas (ESAs)<sup>[34]</sup> are calculated to be 85.5 m<sup>2</sup> g<sup>-1</sup> metal (85.5 m<sup>2</sup> g<sup>-1</sup> Pt) for Pt/C and 74.8 m<sup>2</sup> g<sup>-1</sup> metal (83.2 m<sup>2</sup> g<sup>-1</sup> Pt)

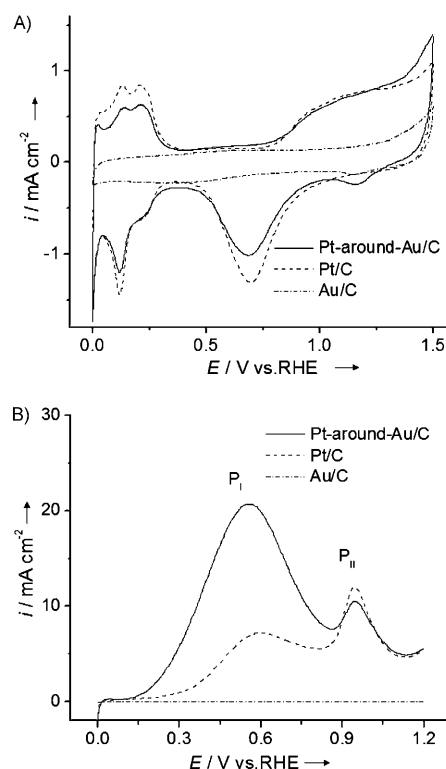


**Figure 3.** A) Cyclic voltammograms in N<sub>2</sub>-saturated 0.5 M H<sub>2</sub>SO<sub>4</sub> and B) polarization curves in N<sub>2</sub>-saturated 0.5 M HCOOH + 0.5 M H<sub>2</sub>SO<sub>4</sub> on Pt/C, Au/C, and Pt-around-Au/C. Scan rate: 50 mV s<sup>-1</sup> (room temperature).

for Pt-around-Au/C. Since Au does not adsorb hydrogen (as shown in Figure 3A),<sup>[33]</sup> the nearly identical ESA values (based on Pt weight) of the two samples indicate that Au NPs have a negligible effect on the electrochemical active sites of Pt NPs in Pt-around-Au nanocomposite, which is different from conventional PtAu NPs.<sup>[18,21]</sup> The electrochemical measurements (Figure 3B) in 0.5 M HCOOH + 0.5 M H<sub>2</sub>SO<sub>4</sub> show that the activity towards formic acid oxidation on Pt-around-Au/C is about 3.0 times that on Pt/C in terms of the peak current density  $i_{P_I}$  (shown in Table S1 in the Supporting Information).

HCOOH oxidation on Pt usually follows the so-called dual pathway.<sup>[17,35]</sup>

I: Direct dehydrogenation producing CO<sub>2</sub>.



II: Dehydration generating CO (poisoning intermediate).



The peak P<sub>I</sub> at 0.58 V (Figure 3B) is related to the direct oxidation of HCOOH to CO<sub>2</sub>; the peak P<sub>II</sub> at 0.95 V is due to the oxidation of the CO<sub>ads</sub> generated from the dissociative adsorption step, the intensity of which indicates the amount of CO adsorbed on Pt.<sup>[2,17]</sup> The higher  $i_{P_I}/i_{P_{II}}$  ratio (2.0 vs. 0.6) combined with the lower onset potential (0.15 vs. 0.29 V) for Pt-around-Au/C versus Pt/C indicates that the Pt-around-Au/C prefers the direct dehydrogenation branch during formic acid oxidation.<sup>[2]</sup> In addition, the amperometric  $i$ - $t$  curves (Figure S4 in the Supporting Information) at a fixed potential

of 0.3 V (the anodic working potential in DFAFCs)<sup>[5]</sup> show that the current density at 3600 s on the Pt-around-Au/C catalyst is 0.094 A mg<sup>-1</sup> metal (5.7 times that on the Pt/C catalyst), which demonstrates that Pt-around-Au/C has much higher electrochemical stability towards formic acid oxidation.<sup>[36]</sup>

As shown in Figure 3B, the intensity of peak P<sub>II</sub> on Pt-around-Au/C is slightly lower than that on Pt/C, thus indicating slightly lower CO adsorption on Pt-around-Au/C, which corresponds to the relative values of Pt ESA in the two samples (CO does not adsorb on the surface of Au<sup>[21]</sup>). So CO formation is not affected by Au NPs in Pt-around-Au/C. This situation is quite different from PtAu alloys and Pd, on which CO formation is almost completely suppressed.<sup>[4,18]</sup> Meanwhile, a slightly higher CO stripping potential on Pt-around-Au/C compared to Pt/C (Figure S5 in the Supporting Information) confirms that Au NPs in Pt-around-Au/C do not facilitate the oxidation of CO. Therefore, the presence of Au has no effect on the dehydration process (pathway II, CO as poisoning intermediate) of HCOOH oxidation on Pt.

On a pure Pt electrode, the rate-determining step for the direct dehydrogenation in formic acid oxidation is the first electron transfer ( $\text{HCOOH} \rightarrow \text{HCOO}_{\text{ads}} + \text{H}^+ + \text{e}^-$ ).<sup>[35,37]</sup> Au is not an effective electrocatalyst towards HCOOH oxidation to CO<sub>2</sub> (Figure S6 in the Supporting Information); instead, it facilitates the first electron transfer during the direct dehydrogenation process of formic acid oxidation.<sup>[38–40]</sup> Therefore, one possible reason for the unexpectedly high activity for HCOOH oxidation on the Pt-around-Au nanocomposite is the efficient spillover of HCOO from Au to the surrounding Pt NPs, where HCOO is further oxidized to CO<sub>2</sub>. The detailed mechanism for enhanced HCOOH oxidation on the Pt-around-Au nanocomposite is currently under investigation.

In conclusion, we have synthesized a novel Pt-around-Au nanocomposite by electrostatic self-assembly. It exhibits significantly enhanced activity and high stability towards formic acid oxidation, which shows a promising application in DFAFCs. The findings in this report are important for the understanding of HCOOH oxidation on a decorated Pt surface, the development of advanced DFAFC anode catalysts, and the synthesis of novel nanocomposites. Considering the important role of binary metal NPs in catalytic systems, this work may also find applications beyond fuel cells.

## Experimental Section

Poly(diallyldimethylammonium chloride) (PDDA, average MW < 100 000), sodium citrate, hexachloroplatinic acid (H<sub>2</sub>PtCl<sub>6</sub>·6H<sub>2</sub>O), chloroauric acid (HAuCl<sub>4</sub>·3H<sub>2</sub>O), and a 5 wt. % Nafion solution were obtained from Sigma–Aldrich.

The preparation of positively charged Pt NPs and negatively charged Au NPs is described in the Supporting Information. Pt-around-Au nanocomposite was synthesized as follows. A solution containing Pt NPs (10 mg) and another one containing Au NPs (1.2 mg) were mixed under vigorous stirring for 10 min. Then Vulcan XC-72R carbon black (44.8 mg, ultrasonicated for 20 min in 2-propanol/H<sub>2</sub>O) was added and the mixture was stirred for 48 h. After that, NaOH (500 mg) was added to increase the ionic strength of the solution and to promote adsorption of the nanocomposite on the carbon support. The resulting catalyst was filtered and washed with

DI water until no Cl<sup>-</sup> was detected and then dried at 90 °C for 3 h in vacuum. A material with 20 wt. % Pt-around-Au/C is obtained. For comparison, 20 wt. % Pt/C (in PDDA solution) and 2 wt. % Au/C (in sodium citrate solution) were prepared by the same method.

The transmission electron microscopy (TEM) images of the catalysts were taken on a JEOL TEM 2010 microscope. X-ray diffraction (XRD) patterns were obtained using a Philips Xpert X-ray diffractometer using Cu<sub>Kα</sub> radiation at  $\lambda = 1.5418 \text{ \AA}$ .

The electrochemical tests were carried out in a standard three-electrode system controlled with a CHI660C station (CH Instruments, Inc., USA) with Pt wire and Hg/Hg<sub>2</sub>SO<sub>4</sub> as the counter electrode and reference electrode, respectively. The related details are provided in the Supporting Information. All the tests were conducted at room temperature. All potentials were reported versus the reversible hydrogen electrode (RHE).

Received: December 11, 2009

Published online: February 23, 2010

**Keywords:** heterogeneous catalysis · nanoparticles · oxidation · platinum · self-assembly

- [1] S. Ha, R. Larsen, R. I. Masel, *J. Power Sources* **2005**, *144*, 28–34.
- [2] N. Kristian, Y. S. Yan, X. Wang, *Chem. Commun.* **2008**, 353–355.
- [3] S. Uhm, H. J. Lee, Y. Kwon, J. Lee, *Angew. Chem.* **2008**, *120*, 10317–10320; *Angew. Chem. Int. Ed.* **2008**, *47*, 10163–10166.
- [4] Y. J. Huang, X. C. Zhou, J. H. Liao, C. P. Liu, T. H. Lu, W. Xing, *Electrochem. Commun.* **2008**, *10*, 621–624.
- [5] X. W. Yu, P. G. Pickup, *J. Power Sources* **2008**, *182*, 124–132.
- [6] N. Tian, Z. Y. Zhou, S. G. Sun, Y. Ding, Z. L. Wang, *Science* **2007**, *316*, 732–735.
- [7] V. Mazumder, S. H. Sun, *J. Am. Chem. Soc.* **2009**, *131*, 4588–4589.
- [8] Y. X. Chen, M. Heinen, Z. Jusys, R. B. Behm, *Angew. Chem.* **2006**, *118*, 995–1000; *Angew. Chem. Int. Ed.* **2006**, *45*, 981–985.
- [9] J. Luo, L. Wang, D. Mott, P. N. Njoki, Y. Lin, T. He, Z. Xu, B. N. Wanjana, I. I. S. Lim, C. J. Zhong, *Adv. Mater.* **2008**, *20*, 4342–4347.
- [10] Y. H. Lin, X. L. Cui, C. Yen, C. M. Wai, *J. Phys. Chem. B* **2005**, *109*, 14410–14415.
- [11] C. W. Xu, H. Wang, P. K. Shen, S. P. Jiang, *Adv. Mater.* **2007**, *19*, 4256–4259.
- [12] J. B. Xu, T. S. Zhao, Z. X. Liang, L. D. Zhu, *Chem. Mater.* **2008**, *20*, 1688–1690.
- [13] W. P. Zhou, A. Lewera, R. Larsen, R. I. Masel, P. S. Bagus, A. Wieckowski, *J. Phys. Chem. B* **2006**, *110*, 13393–13398.
- [14] N. Hoshi, K. Kida, M. Nakamura, M. Nakada, K. Osada, *J. Phys. Chem. B* **2006**, *110*, 12480–12484.
- [15] J. Solla-Gullon, V. Montiel, A. Aldaz, J. Clavilier, *Electrochem. Commun.* **2002**, *4*, 716–721.
- [16] P. K. Babu, H. S. Kim, J. H. Chung, E. Oldfield, A. Wieckowski, *J. Phys. Chem. B* **2004**, *108*, 20228–20232.
- [17] S. Park, Y. Xie, M. J. Weaver, *Langmuir* **2002**, *18*, 5792–5798.
- [18] S. Zhang, Y. Y. Shao, G. P. Yin, Y. H. Lin, *J. Power Sources* **2010**, *195*, 1103–1106.
- [19] Z. Peng, H. Yang, *Nano Res.* **2009**, *2*, 406–415.
- [20] B. Lim, M. J. Jiang, P. H. C. Camargo, E. C. Cho, J. Tao, X. M. Lu, Y. M. Zhu, Y. N. Xia, *Science* **2009**, *324*, 1302–1305.
- [21] J. Zhang, K. Sasaki, E. Sutter, R. R. Adzic, *Science* **2007**, *315*, 220–222.
- [22] H. J. Lee, S. E. Habas, G. A. Somorjai, P. D. Yang, *J. Am. Chem. Soc.* **2008**, *130*, 5406–5407.
- [23] M. E. Leunissen, C. G. Christova, A. P. Hynninen, C. P. Royall, A. I. Campbell, A. Imhof, M. Dijkstra, R. Van Roij, A. Van Blaaderen, *Nature* **2005**, *437*, 235–240.

- [24] B. A. Grzybowski, A. Winkleman, J. A. Wiles, Y. Brumer, G. M. Whitesides, *Nat. Mater.* **2003**, 2, 241–245.
- [25] A. M. Kalsin, M. Fialkowski, M. Paszewski, S. K. Smoukov, K. J. M. Bishop, B. A. Grzybowski, *Science* **2006**, 312, 420–424.
- [26] J. Kolny, A. Kornowski, H. Weller, *Nano Lett.* **2002**, 2, 361–364.
- [27] E. V. Shevchenko, D. V. Talapin, N. A. Kotov, S. O'Brien, C. B. Murray, *Nature* **2006**, 439, 55–59.
- [28] S. Zhang, Y. Y. Shao, G. P. Yin, Y. H. Lin, *J. Mater. Chem.* **2009**, 19, 7995–8001.
- [29] A. Roucoux, J. Schulz, H. Patin, *Chem. Rev.* **2002**, 102, 3757–3778.
- [30] Q. Zhu, S. H. Zhou, X. Q. Wang, S. Dai, *J. Power Sources* **2009**, 193, 495–500.
- [31] V. Tohver, J. E. Smay, A. Braem, P. V. Braun, J. A. Lewis, *Proc. Natl. Acad. Sci. USA* **2001**, 98, 8950–8954.
- [32] Y. Y. Shao, G. P. Yin, Y. Z. Gao, P. F. Shi, *J. Electrochem. Soc.* **2006**, 153, A1093–A1097.
- [33] I. S. Park, K. S. Lee, D. S. Jung, H. Y. Park, Y. E. Sung, *Electrochim. Acta* **2007**, 52, 5599–5605.
- [34] Z. H. Wen, Q. Wang, J. H. Li, *Adv. Funct. Mater.* **2008**, 18, 959–964.
- [35] J. D. Lovic, A. V. Tripkovic, S. L. J. Gojkovic, K. D. Popovic, D. V. Tripkovic, P. Olszewski, A. Kowal, *J. Electroanal. Chem.* **2005**, 581, 294–302.
- [36] R. F. Wang, S. J. Liao, S. Ji, *J. Power Sources* **2008**, 180, 205–208.
- [37] M. D. Macia, E. Herrero, J. M. Feliu, *J. Electroanal. Chem.* **2003**, 554, 25–34.
- [38] J. Xiang, B. L. Wu, S. L. Chen, *J. Electroanal. Chem.* **2001**, 517, 95–100.
- [39] M. Ojeda, E. Iglesia, *Angew. Chem.* **2009**, 121, 4894–4897; *Angew. Chem. Int. Ed.* **2009**, 48, 4800–4803.
- [40] D. Zhao, Y. H. Wang, B. Q. Xu, *J. Phys. Chem. C* **2009**, 113, 20903–20911.